Analytical Methods

Accepted Manuscript

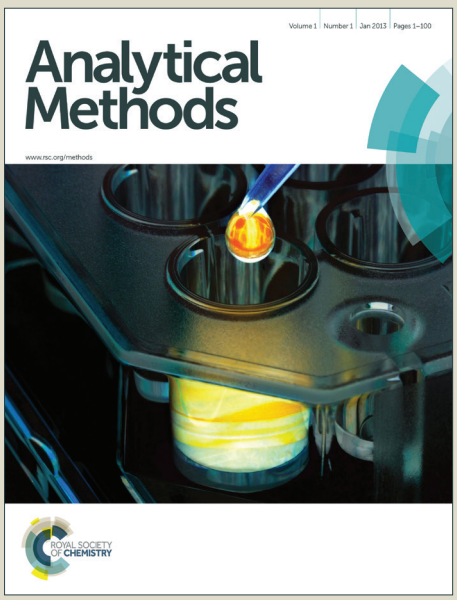

ROYAL SOCIETY OF CHEMISTRY

www.rsc.org/methods

Journal Name

RSCPublishing

ARTICLE

Preparation of a reduced graphene oxide/poly-l-glutathione nanocomposite for electrochemical detection of 4-aminophenol in orange juice samples

Cite this: DOI: 10.1039/x0xx00000x

Received 00th January 2012,
Accepted 00th January 2012

DOI: 10.1039/x0xx00000x

www.rsc.org/

A.T.Ezhil Vilian,[a,c] Vediyappan Veeramani,[a] Shen-Ming Chen,[a,*] Rajesh Madhu,[a] Yun Suk Huh,[b,*] Young-Kyu Han,[c,*]

A novel electrochemical sensor, 4-aminophenol (4-AP), was generated by electrodeposition of poly-L-glutathione (P-L-GSH) onto reduced graphene oxide (RGO) to form a RGO/P-L-GSH composite matrix on a glassy carbon electrode (RGO/P-L-GSH/GCE). The morphology and structure of RGO/P-L-GSH modified GCE were characterized by scanning electron microscopy (SEM), FT-IR spectroscopy and electrochemical impedance spectroscopy. As an electrochemical sensor, the RGO/P-L-GSH modified GCE composite exhibited strong catalytic activity toward the oxidation of 4-AP by cyclic voltammetry (CV) and chronoamperometry. Furthermore, the electrochemical sensor exhibited an excellent current response for 4-AP over a wide linear range of 0.4 to 200 µM (R^2 = 0.9934) with a lower detection limit (LOD) of 0.03 µM (S/N = 3), as well as a sensitivity of 27.2 (µA μM^{-1} cm^{-2}) and excellent selectivity, reproducibility and stability. The electrochemical sensor demonstrated good anti-interference ability in the presence of glucose, fructose, paracetamol, ethanol, l-isoluecine, l-histidine, l-cysteine, dopamine, l-serine, l-tyrosine, phenylalanine, urea, hydrogen peroxide, K^+, Ca^{2+}, Na^+, F^-, SO_4^{2-}, Cu^{2+}, Fe^{3+}, Zn^{2+}, SO_4^{2-}, SO_3^{2-}, Cl^-, folic acid and ascorbic acid. The proposed electrochemical method was successfully applied to produce a sensor for the detection of 4-AP in juice and water samples.

*Corresponding authors:

[a,*] *Electroanalysis and Bioelectrochemistry Lab, Department of Chemical Engineering and Biotechnology,National Taipei University of Technology, Taipei 10608, Taiwan* Fax: (886)-2-27025238. E-mail: smchen78@ms15.hinet.net (S.M.Chen),

[b,*] *Department of Biological Engineering, Biohybrid Systems Research Center (BSRC), Inha University, Incheon 402-751, Republic of Korea*. Fax: +82 32 872 4046. E-mail: yunsuk.huh@inha.ac.kr (Y.S. Huh),

[c,*] *Department of Energy and Materials Engineering, Dongguk University-Seoul, Seoul, Republic of Korea*. Fax: +82 2 2268 8550. E-mail : ykenergy@dongguk.edu (Y.-K. Han).

Journal Name

RSCPublishing

ARTICLE

1. Introduction

Graphene comprised of a single layer of carbon atoms with a honeycomb two-dimensional lattice structure has been produced [1] and received a great deal of attention as a potential carbon material over the last decade because of its superior mechanical strength, low density and high heat conductance. Many possible applications of graphene-based composites have been investigated, including as components of batteries, fuel cells, drug delivery systems and biosensors.[2,3]

Several researchers have recently suggested other possible methods for synthesis of graphene nanosheets including the mechanical exfoliation of graphite, chemical reduction of graphite oxide (GO), chemical vapour deposition, and electrochemical methods.[4,5] Moreover, chemical reduction of GO is a valuable approach because it is low lost, has high production capacity and is non-toxic. However, the reductant most commonly used for this technique is hydrazine hydrate, which is highly toxic, dangerously unstable and harmful to humans and the environment.[6] In this study, mild electrochemical reduction techniques were employed to reduce the GO and obtain graphene nanosheets to decrease toxicity and danger. However, an efficient method for the preparation of electrochemically reduced graphene oxide (RGO) films with a lower oxygen content has yet to be developed. [7]

4-AP (p-aminophenol; 4-AP) is an essential basic material commonly used for the production of dyes, polymers and pharmaceuticals.[8,9] However, 4-AP is a hydrolytic product of acetaminophen that has serious nephrotoxic and teratogenic effects and has been observed as a synthetic intermediate.[10] 4-AP can also be synthetically produced by several methods, including rearrangement of phenylhydroxylamine in a sulfuric acid solution.[11] 4-AP is used in the manufacture of azo, sulfur, acid wool and leather dyes, which are toxic and irritating to the eyes, skin and respiratory system. In addition, this compound poses a risk of irreversible effects on human health, specifically the blood and kidneys.[12] Various strategies have been developed for the detection of 4-AP including chromatography, capillary electrophoresis (CE), high performance liquid chromatography, and microfluidic device electrochemical detection. Among these, electrochemical techniques provide the best opportunity for the development of portable, economic, sensitive and rapid methodologies for the detection of 4-aminophenol.[13-17]

There have also been several studies of 4-AP oxidation using different analytical measurements. Huanshun Yin et al. fabricated a graphene-chitosan composite film modified glassy carbon electrode (GCE) and used differential pulse voltammetry to measure the 4-AP in a 0.1M pH 6.3 phosphate buffer solution.[18] Fan et al. investigated the use of electrochemical sensors based on graphene-polyaniline (GR-PANI) nanocomposites to detect 4-AP by differential pulse voltammetry.[19] Neto et al. demonstrated the performance of a hemin-modified molecularly imprinted polymer (MIP) used as an amperometric sensor for the detection of 4-AP.[20] Shiroma et al. developed a sensitive microfluidic paper-based device for electrochemical detection of paracetamol and 4-AP.[21] De Bleye employed a quantified 4-AP in a pharmaceutical formulation containing acetaminophen using surface-enhanced Raman scattering.[22] In addition, Wang et al. described a high-performance photo electrochemical sensor for the detection of 4-AP based on an MIP/CdS-GR modified electrode.[23] However, there is increasing demand for simpler analytical devices that can provide rapid results and provide uncomplicated analysis without the demand for a full laboratory setting. This has driven the demand for the use of materials with reduced cost that can provide various advantages to their applied device.

To the best of our knowledge, this is the first investigation of use of GSH deposited on RGO with glassy carbon electrode modified films as enhanced materials for the detection of 4-AP. The morphological, structural and electrochemical properties of the prepared RGO/P-L-GSH nanomaterials have been characterized in detail. The fabricated 4-AP sensor demonstrated a wide linear range of 0.4 to 200 μM and a detection limit of 0.03 μM, as well as good anti-interference utility, reusability, and long-term storage stability. The performance of the RGO/P-L-GSH modified GCE demonstrated remarkably high

sensitivity and very low LOD for amperometric determination of 4-AP when compared to most other sensors reported in recent years. The 4-AP sensor was also applied for analysis of juice and water samples, and the results showed it was useful in practical applications.

2. Experimental Section

2.1. Reagents

The graphite (powder, <20 lm), L-glutathione, 4-aminophenol, Na_2HPO_4 and NaH_2PO_4, were received from the Sigma Chemical Company. In addition a 0.05 M phosphate buffer solution (PBS, pH 7) was used as the supporting electrolyte. Other chemicals were of analytical reagent grade, and all aqueous solutions were prepared with double distilled water for use in the experiments.

2.2. Apparatus

All the electrochemical measurements were executed on a CHI 405A electrochemical workstation (Shanghai Chenhua Instrument, China). A conventional three-electrode system was used with an RGO/P-L-GSH film modified electrode as the working electrode, a platinum wire as the auxiliary electrode and a saturated Ag/AgCl as the reference electrode. Electrochemical impedance spectroscopy (EIS) was carried out in a frequency range of 0.1 Hz to 1 MHz with a ZAHNER instrument (Kroanch, Germany). Scanning electron microscopy (SEM) was performed on a Hitachi S-3000 H scanning electron microscope (Japan Electron Company, Japan). TEM (JEOL, JEM-2010F) was characterized at an accelerating voltage of 200 kV. FT-IR spectra was performed using a Nicolet 6700 FT-IR spectrometer (Thermo Fisher Scientific Inc., USA).

2.3. Preparation of the modified electrode

Prior to modification, the GCE was polished with 0.05 μm α-Al_2O_3 powder slurries to get a mirror-like surface, and then sonicated sequentially in acetone, HNO_3 (1:1, v/v), and double distilled water for 2 min. The GO was synthesized according to the previously described procedure.[24] A typical schematic representation of the fabrication of the RGO/P-L-GSH modified electrode is shown in Scheme. 1. After fabrication, 5 μL of GO suspension was directly applied on the GCE surface and it was then allowed to dry at room temperature for 3 h. The GO modified GCE was immersed into a N_2 saturated PBS (pH 5.0) solution. Subsequently, the GO modified electrode was then electrochemically reduced to RGO by performing 5 successive cycles of cyclic voltammograms (CVs) in the potential range between 0 and -1.5 V at a scan rate of 50 mV s^{-1} (Fig.1A).During the first a large cathodic peak appears at -1.4 V, which might be due to the reduction oxygen functional groups (such as epoxide, carboxyl, and hydroxyl) present on the surface of GO with an onset potential of -0.8 V. After few cycles, this cathodic peak disappeared completely, attributed to the complete reduction of oxygen functional groups present on the surface of GO basal plane and to retain the lattice of graphene.[25] The RGO modified GCE was then allowed to dry at room temperature for few minutes.Then the RGO modified electrode was transferred to an electrochemical cell with 10 ml of 0.05 M PBS buffer solution (pH 6) containing 10 mM of GSH. The RGO modified electrodes were subjected to 10 successive cycles of CVs in the potential range between -1.5 to + 2.0 V (vs. the Ag/AgCl reference electrode at a scan rate of 100 mVs^{-1}). In this process, L-GSH monomer was oxidized to form a-amino free radical at a higher positive potential, which can be easily combine with RGO modified GCE surface (Fig.1B). However, the fabarication RGO/P-L-GSH modified GCE bind with positively charged GSH was to enhance the immobilization of negatively charged RGO on GCE electrode surface through the electrostatic attraction. The RGO/P-L-GSH modified GCE was then gently rinsed with distilled water to remove any loosely bound RGO/P-L-GSH before being dried at room temperature. Finally, the fabricated RGO/P-L-GSH modified GCE was used for electrochemical experiments. It was immersed in PBS 7 at 4 °C when not in use. All the electrochemical studies were carried out in the presence of a N_2 atmosphere.

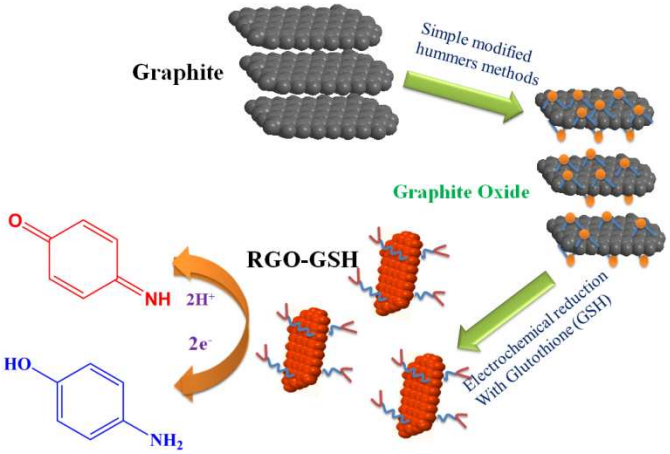

Scheme 1. Schematic illustration of the preparation of RGO/P-L-GSH modified GCE.

3. Results and discussion

3.1 Morphology and structural characterization

The surface morphology of the RGO and RGO/P-L-GSH composite were studied directly by SEM. As observed in Fig. 2A, the RGO exhibited a typical flake-like shape with slight wrinkles on the surface. Additionally, the deposition of GSH did not change the morphology of the RGO significantly (Fig. 2B). The as prepared RGO/P-L-GSH composite shows a typical thin wrinkled layered structure. Observation of the edge of the nanosheet confirmed the layered structure of the RGO.

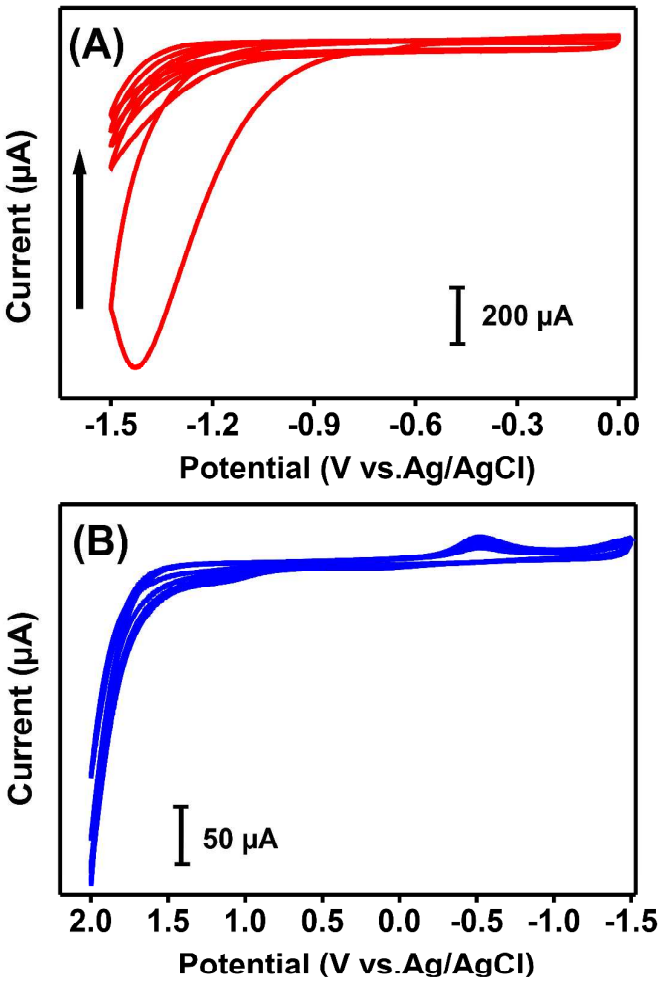

Fig. 1. (A) Electrochemical reduction of GO modified GCE for 5 successive cyclic voltammograms was performed at 0 to -1.5 V in pH 5 solution at a scan rate of 50 mV s^{-1}. (B) Cyclic voltammograms of the electro-polymerization process of P-L-GSH from 1 to 10 cycles (10 mM of GSH in pH 6.0 PBS), scan rate: 100 mV s^{-1}.

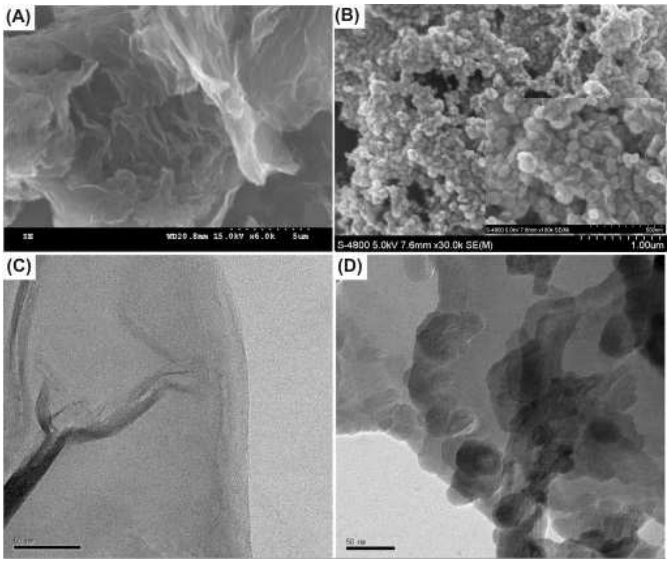

Fig. 2. SEM images of (A) RGO and (B) RGO/P-L-GSH modified films and TEM images of (C) RGO and (D) RGO/P-L-GSH modified films.

The morphologies of the RGO and RGO/P-L-GSH films were analyzed by TEM. RGO (Fig. 2C) had a wrinkled paper-like structure with irregular size. These wrinkles are essential for preventing the aggregation of RGO during drying and providing a high surface area. As shown in Fig. 2D, P-L-GSH were bound on the RGO surface with a dense distribution, illustrating the strong interaction between P-L-GSH and RGO. These results demonstrated that P-L-GSH were successfully deposited onto RGO to form a RGO/P-L-GSH film.

The FT-IR spectra of GO and GO after reduction by the P-L-GSH are shown in Fig. 3A. The characteristic absorption bands of the GO, including C=O stretching vibration, appear at 1746 cm^{-1}, while for O–H, stretching and deformation vibration appear at 3420 cm^{-1} and 1395 cm^{-1}, respectively, as shown in curve a.[26,27] Conversely, as shown in the RGO/P-L-GSH nanocomposite (curve b), aromatic C=C stretching vibration was exhibited at 1625 cm^{-1}, with peaks at 1220 cm^{-1} and 1053 cm^{-1} corresponding to the epoxy C–O stretching vibration and the alkoxy C–O stretching vibration, respectively. While being reduced by L-glutathione, the peaks for the oxygen functional groups gradually decreased with

reaction time, and some disappeared completely. These results demonstrate that most oxygen functionalities of the GO were removed. This could be attributed to the synergistic effect of hydrogen bonding and electrostatic interaction between GSH on the GO surfaces. [28,29]

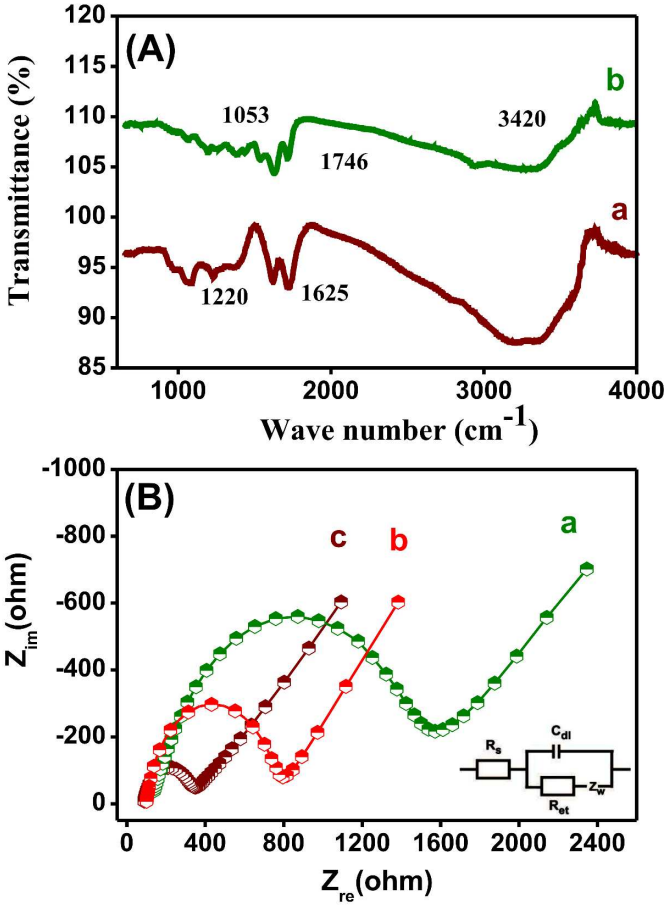

Fig. 3. (A) FTIR spectra of (a) GO, (b) RGO/P-L-GSH modified film, and (B) Nyquist plots for (a) GO/GCE, (b) bare GCE, and (c) RGO/P-L-GSH modified film for 5 mM $Fe(CN)_6^{3-/4-}$ in a 0.05 M PBS (pH 7) solution containing 0.1 M KCl. Amplitude: 5 mV; frequency: 0.1 Hz to 1 MHz. The bottom right inset shows the Randles equivalence circuit for the aforementioned electrodes.

3.2 Electrochemical behavior of the RGO-GSH modified electrode

EIS is one of the most powerful tools for probing the features of surface modified electrodes. The impedance spectra include a semicircular portion at higher frequencies corresponding to the electron-transfer-limited process and a linear part at the lower frequency range representing the diffusion-limited process. Fig. 3B shows the EIS of the bare GCE, GO/GCE and RGO/P-L-GSH modified electrodes in a 5 mM $Fe(CN)_6^{3-/4-}$ and 0.05 M PBS (pH 7) solution containing 0.1 M KCl with frequency sweeping from 0.1 Hz to 1 MHz. The EIS results of different electrodes, which were fitted based on the randles equivalent circuit, are shown in the inset of Fig. 3B. This equivalent circuit consists of the ohmic resistance of the electrolyte (R_s), the Warburg impedance (Z_w), the electron transfer resistance (R_{et}) and an interfacial capacitance (C_{dl}). For the bare GCE (curve b), we obtained an Ret value of the semicircle of 806 Ω. After the GO was dropped onto the bare GCE (curve a), the R_{et} value increased to 1589 Ω, suggesting that the addition of a GO composite film can decrease the rate of electron transfer. After the GSH was used to modify the RGO/GCE electrode (curve c), the diameter of the semicircle decreased owing to the formation of a RGO/P-L-GSH modified electrode, while the R_{et} decreased to 378.9 Ω. This may indicate that the RGO/P-L-GSH modified electrode film provided higher electron conduction pathways than the GO film or the bare GCE.

Comparisons of the electrochemical CVs of the bare GCE, RGO/GCE, and RGO/P-L-GSH modified electrodes are shown in Fig. 4A. The samples were characterized using CV and EIS in 5 mM $Fe(CN)_6^{3-/4-}$ in a 0.05 M PBS (pH 7) solution containing 0.1 M KCl at a scan rate of 100 mV s^{-1}. Modification of the GO/GCE led to a remarkable reduction in the ΔEp value for the $Fe(CN)_6^{3-/4-}$ redox couple to 140 mVs^{-1} (curve c), which was accompanied by enhancement of the CV response, indicating that the GO film can promote electron transfer and facilitate redox reaction of the $Fe(CN)_6^{3-/4-}$ probe. At the RGO/P-L-GSH modified electrodes, a pair of redox waves was measured with a peak-to-peak separation (ΔEp) of 80 mV s^{-1} (curve b). This value was much lower than that obtained for the GO/GCE and bare GCE (98 mV, curve a). We propose that the $Fe(CN)_6^{3-/4-}$ redox coupling on the RGO/P-L-GSH modified electrodes is characterized by fast electron transfer kinetics, which is feasible due to the presence of P-L-GSH on the RGO/GCE surface.

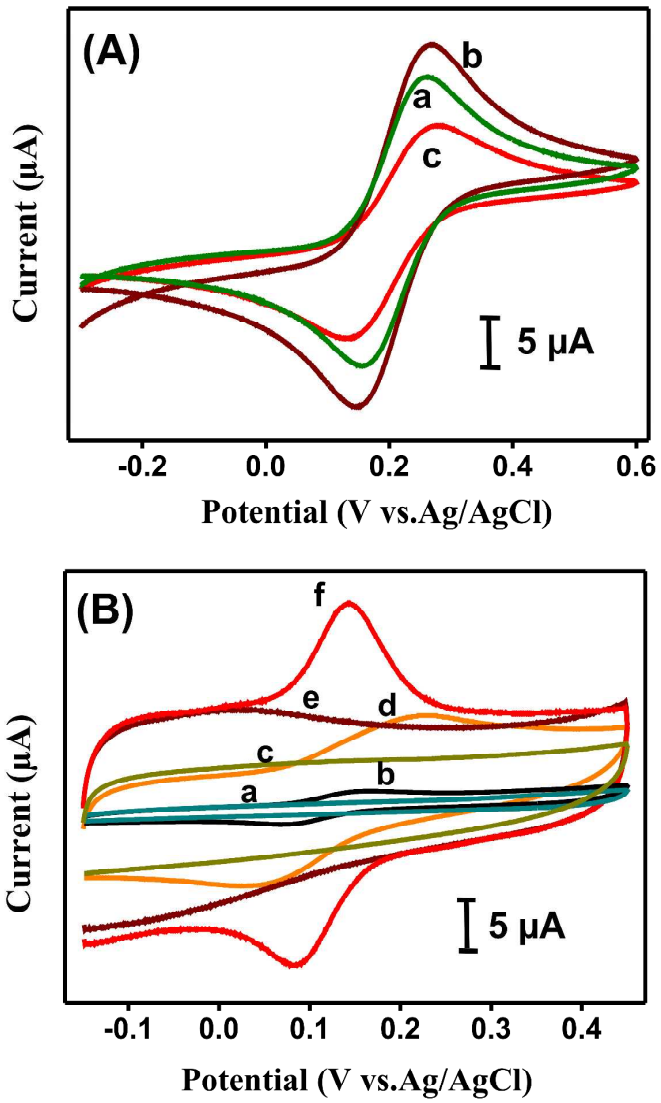

Fig. 4. (A) Cyclic voltammograms of the (a) bare GCE, (b) RGO/P-L-GSH/GCE. and (c) GO modified GCE electrodes in 5 mM $Fe(CN)_6^{3-/4-}$ in a 0.05 M PBS (pH 7) solution containing 0.1 M KCl. (B) Cyclic voltammograms of 1 × 10^{-4} M 4-AP (presence/absence) for the (a) & (b) bare GCE, (c) & (d) RGO/GCE, (e) & (f) RGO/P-L-GSH modified GCE electrodes in PBS (pH 7). Scan rate: 100 mV s^{-1}.

Fig. 4B shows the CVs of bare/GCE, RGO/GCE and RGO/P-L-GSH modified GCE electrodes with and without 1×10^{-4} M of 4-AP in a 0.05 M PBS solution (pH 7) at 100 mV s^{-1}. There were no evident redox peaks observed at the bare GCE (curve a), RGO/GCE (curve c) and RGO/P-L-GSH modified GCE electrodes in 0.05 M PBS solution (pH 7); however, a high specific background current was observed for the RGO/P-L-GSH modified GCE (curve e), indicating that the presence of RGO resulted in a clear increase in the background current due to the increased active electrode surface area. When 1×10^{-4} M 4-AP was added, the bare GCE (curve b) showed an irreversible electrochemical behaviour with relatively weak redox current peaks, Epa (anodic peak potential) of 0.190 V and Epc (cathodic peak potential) of 0.049 V. The 4-AP depicts a pair of well defined redox peaks on the RGO/GCE with an Epa of 0.227 V and an Epc at of 0.097 V (curve d). The bare and RGO modified GCE had poor sensitivity for 4-AP, and the anodic peak currents were relatively small throughout the RGO surface. Additionally, the anodic peaks of 4-AP for the electrochemically deposited RGO-P-L-GSH modified film were investigated at 0.134 and 0.092 V. There was a two-fold increase in the anodic peak current of 4-AP over that of the bare GCE and RGO modified GCE electrodes. The electrochemically deposited RGO/P-L-GSH modified GCE had a well-defined oxidation peak of 4-AP at 0.134 with a peak to peak separation (ΔEp) of 42 (see Table 1). The smaller ΔEp values were indicative of the faster electron transfer of 4-AP, and the decreasing overpotential could be attributed to the RGO/P-L-GSH modified electrode surface. These results demonstrate that the ability to greatly accelerate the electron-transfer process and larger electroactive area, RGO/P-L-GSH modified GCE were present excellent higher catalytic efficiency.

3.3 Influence of scan rate on electro catalysis of 4- aminophenol

The effects of the scan rate (υ) on the electrochemical behaviour of 1×10^{-4} M 4-AP on the RGO/P-L-GSH modified GCE were investigated by CV. As shown in Fig. 5A, both the anodic peak currents (I_{pa}) and cathodic peak currents (I_{pc}) of 4-AP showed good linear relationships with the square root of the scan rate ($\upsilon^{1/2}$) at 0.01 to 0.1 mV/s. The regression equations for 4-AP can be expressed as Ipa = -20.812 $v^{1/2}$ - 2.128 (µA, $V^{1/2}/s^{1/2}$,R^2 = 0.9905) and Ipc (µA) = 21.705 $v^{1/2}$ + 2.1093 (µA, $V^{1/2}/s^{1/2}$,R^2 = 0.9907). These results demonstrated that the electrochemical oxidation of 4-AP on the RGO/P-L-GSH modified GCE was a typical diffusion-controlled process.[30]

3.4 Electro catalysis of the RGO/P-L-GSH modified electrode

Fig. 5B displays the chronoamperogram curves of a rotating (1200 rpm) RGO/P-L-GSH modified electrode measured at pH 7 after successive addition of 4-AP at an applied potential of +0.15 V vs. Ag/AgCl. When a proper of 4-AP was added into the pH 7 buffer solution, the Ipa peak currents increased steeply, resulting in a maximum steady-state current within 3 s. These findings indicated

that the RGO/P-L-GSH modified electrode was able to catalyze 4-AP oxidation efficiently. A linear relationship between Ipa peak current vs. 4-AP concentration was obtained (Fig. 5B inset) using 0.4 to 200 μM 4-AP. The regression equation was I (μA) = 1.904x + 0.2489 [4-AP] (μM) (R^2 = 0.9934) and the LOD was calculated to be 0.03 μM (S/N = 3). The sensitivity of the RGO/P-L-GSH modified electrode was 27.2 (μA μM^{-1} cm^{-2}). The analytical performance of the modified electrode for determination of 4-AP was compared with that of other modified electrodes previously reported in the literature (see Table 2). The results indicate a comparable, or in some cases better performance of the proposed sensor to that of other modified electrodes for determination of 4-AP, while the LOD for 4-AP was among the lowest concentrations reported in the literature. The linear range of the reported 4-AP sensor is greater than that reported in several previous studies, demonstrating the excellent catalytic ability of the RGO/P-L-GSH nanostructured surface of the modified electrode. These findings indicate that it could be a good option for 4-AP detection.

Table 1 Electrochemical parameters of 1×10^{-4} M of 4-AP on different electrodes.

Electrodes	Epa/V	Epc/V	Ipa	Ipc	ΔEp	$E^{o\prime}$
Bare/GCE	0.190	0.049	1.216	1.411	0.141	0.1195
RGO/GCE	0.227	0.097	5.123	3.925	0.130	0.162
RGO/P-L-GSH/GCE	0.134	0.092	10.83	11.41	0.042	0.113

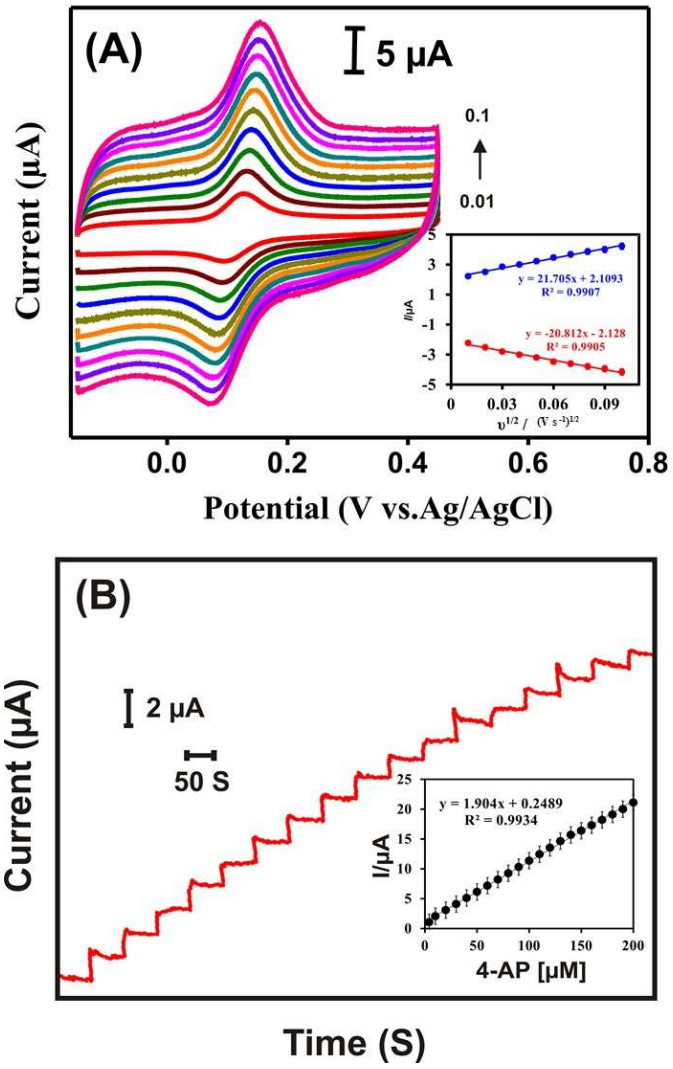

Fig. 5. (A) CVs of the RGO/P-L-GSH modified GCE in 0.05 M deoxygenated PBS (pH 7) containing 1×10^{-4} M 4-AP obtained at different scan rates (from inner to outer: 0.01 to 0.1 V s^{-1}). Inset: anodic and cathodic peak current vs. scan rate. (B) Amperometric response of RGO/P-L-GSH modified rotating disc electrodes to successive 4-AP injections at an applied potential of +0.15 V in 0.05M PBS (pH 7). Inset: calibration plot between current and 4-AP concentration.

The effect of solution pH (for a range from 3 to 11) on the response of 4-AP for the RGO/P-L-GSH modified GCE is shown in Fig. 6A. There was a slow increase in the anodic peak current as pH increased from 3 to 7, while the anodic peak decreased from pH 7.0 to 11. In addition, we inverted the relationship between pH and the anodic peak potential (Epa) of 4-AP, which revealed a negative shift in the anodic peak potential as pH increased from 3 to 11 for 4-aminophenol. The equation describing the change in peak potential

with pH for 4-AP was Epa = -0.0515 pH + 0.0567 (R^2 = 0.999). In addition, the slopes of the regression functions were close to the theoretical value of 58.5 mV pH^{-1}, indicating that the number of electrons and protons taking part in the RGO/P-L-GSH modified GCE electrode reaction was equal. Therefore, a pH of 7 was selected as the optimal value for the detection of 4-AP. Thus, the electrochemical oxidation of 4-AP at the RGO/P-L-GSH film should be a two-electron and two-proton process as illustrated in Scheme 2.[31]

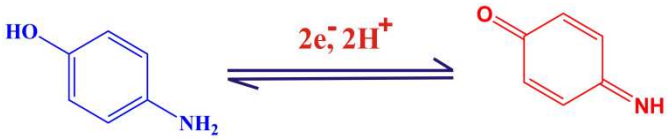

Scheme 2. Possible electro oxidation reaction mechanism of 4-AP

3.5 Selectivity of the sensor

Interference studies were carried out to investigate the selectivity of the sensor under optimum conditions. A 100 µM concentration of 4-AP in 0.05 M phosphate buffer solution (pH 7) was used to evaluate the selectivity of the sensor in the presence of 40 µM analytes such as glucose, paracetamol, fructose, ethanol, l-isoluecine, l-histidine, l-cysteine, l-serine, l-tyrosine, phenylalanine, urea, hydrogen peroxide, K^+, Ca^{2+}, Na^+, F^-, SO_4^{2-}, Cu^{2+}, Fe^{3+}, Zn^{2+}, SO_4^{2-}, SO_3^{2-}, Cl^-, folic acid, dopamine, paracetamol and ascorbic acid. Our findings indicated that the tested substances did not significantly interfere with the results.

3.6 Reproducibility, repeatability and stability

The repeatability of the RGO/P-L-GSH modified GCE electrode was investigated by voltammetry with 1 × 10^{-4} M 4-AP in 0.05 M PBS (pH 7) for eight successive measurements. The relative standard deviation (RSD) was 1.45% in 4-aminophenol. These experimental results confirm that the RGO/P-L-GSH modified GCE electrode had good repeatability. The fabrication reproducibility was studied by measuring 1 × 10^{-4} M 4-AP with five RGO/P-L-GSH modified GCE electrodes that were fabricated independently under the same conditions. The RSD was 4.1% for 1 × 10^{-4} M 4-AP. To demonstrate the stability of the RGO/P-L-GSH modified electrode, 100 cycles of CVs were carried out using a 1 × 10^{-4} M 4-AP solution in pH 7 PBS at the RGO/P-L-GSH modified GCE (See Fig. 6C and D). The experimental results showed satisfactory reproducibility of the fabrication protocol.

3.7 Analysis of 4-AP in juice and water samples

We investigated the application of the developed method for measurement of 4-AP in juice and various water samples spiked with known amounts of 4-AP. The amounts of 4-AP in the samples were determined using the standard addition method and summarized in Table 3. The obtained recoveries were 98.4-99%, 99.1-99.6%, and 99.2–99.7%. These findings confirm the feasibility of the fabricated RGO/P-L-GSH modified GCE electrode for measurement of 4-AP in juice and water samples.

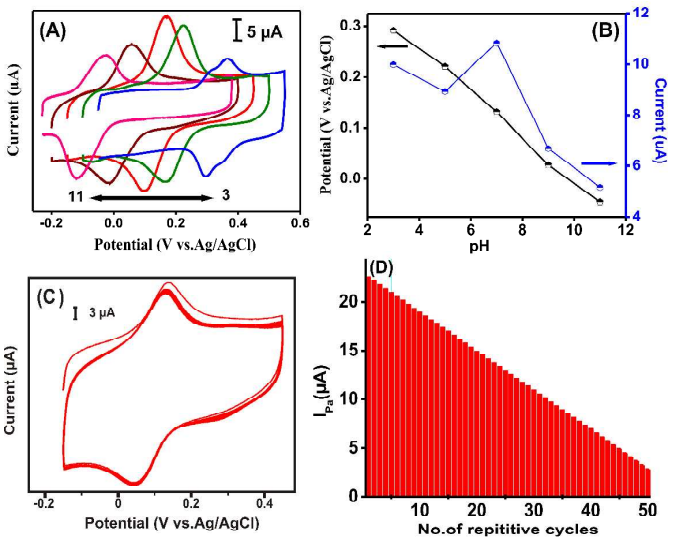

Fig. 6. (A) CVs for 1 × 10^{-4} M 4-AP at the RGO/P-L-GSH modified GCE with different pHs = 3.0, 5.0,7.0, 9.0, and 11. (B) The relationship of peak potential (black) and peak current (blue) with pH. (C) CVs of RGO/P-L-GSH modified GCE for 100 multiple cycles in the presence of 1 × 10^{-4} M 4-AP in 0.05M PBS (pH 7) at a scan rate of 100 mV s^{-1}. (D) Number of repetitive cycles vs. Ip.

Table 2. Comparison of analytical parameters for detection of 4-AP over various modified electrodes.

Modified electrode	Analytical methods	Sensitivity	Linear ranges (μM)	LOD (μM)	Ref
Carbon ionic liquid electrode	DPV	-	0.3-1000	0.1	[17]
Graphene-chitosan/GCE	DPV	-	0.2-550	0.057	[18]
Graphene-polyaniline / GCE	DPV	177,604.2 ($\mu A\ mM^{-1}\ cm^{-2}$)	0.2-20, 20-100	0.065	[19]
ERGO/GCE	DPV	-	0.01-10	0.0029	[30]
mesoporous silica-modified CPE	DPV	-	0.23- 28	0.092	[31]
Poly [N-vinylcarbazole-co-vinylbenzene sulfonic acid]/ carbon fibre microelectrode	CV	-	-	1.00	[32]
Single-wall carbon nanotubes/ poly(4-aminopyridine)	CV	-	0.2-100	0.06	[33]
Poly(3,4-ethylenedioxythiophene) (PEDOT)-modified GCE	DPV	-	4-320	1.2	[34]
Screen-printed carbon electrodes	NPV	-	0.2-200	0.05	[35]
NH_2-SBA-15/CPE	DPV	-	0.1-12	0.02	[36]
25,26,27,28-tetrahydroxycalix[4]arene (CAL4) /Amberlite XAD-16	Fibre-optic reflectance	-	4.6 - 320	1.0	[37]
2,2-(1,4-Phenylenedivinylene)bis-8-hydroxyquinoline / XAD-7	Fibre-optic reflectance	-	0.92- 20	0.18	[38]
Hemin-modified molecularly imprinted polymer	Amperometry	-	10 - 90	3.00	[39]
Molecularly imprinted polypyrrole/CdS-graphene/FTO	Photoelectrochemistry	-	0.05- 3.5	0.023	[40]
RGO/P-L-GSH/ GCE	Amperometry	27.2 ($\mu A\ \mu M^{-1}\ cm^{-2}$)	0.4-200	0.03	**This work**

Table 3. Determination of 4-AP in juice and water samples (n = 3).

Samples	Spiked [μM]	Found [μM]	RSD (%)	Recovery rate (%)
Orange juice	5	4.94±0.12	3.56 ±0.08	98.4
	10	9.96±0.14	2.14 ±0.06	99
Lake water	5	4.92±0.14	3.66 ± 0.13	99.1
	10	9.6±0.13	3.16 ±0.11	99.6
River water	5	4.86±0.22	2.56 ±0.14	99.2
	10	9.2±0.18	3.08 ±0.16	99.7

4. Conclusion

We described a simple method for fabrication of a novel 4-AP sensor based on the as-synthesized RGO/P-L-GSH modified GCE. The RGO/P-L-GSH modified GCE was investigated and characterized by SEM,TEM,EIS and FT-IR. The results revealed a nanostructure with a large effective surface area that allows it to function as an electron transfer medium and enhances charge transfer rate. The RGO/P-L-GSH modified GCE electrode exhibits a high sensitivity and wide linear range of 0.4 to 200 μM for 4-AP response. The flexible electrochemical sensor based on RGO/P-L-GSH modified GCE is useful for determination of 4-AP and has many desirable properties, including high sensitivity, rapid charge transfer rate, wide linear range, low detection limit, long-term storage ability and good anti-interference ability. Accordingly, it has many promising prospective uses in the field of flexible electronics. Additionally, our electrochemical sensor was successfully employed to detect 4-AP in juice and water samples.

3. Acknowledgement

The authors gratefully acknowledge the Ministry of Science and Technology, Taiwan (Republic of China) and a National Research Foundation of Korea (NRF) grant by the Korean Government Ministry of Education, Science and Technology (MEST) (2010-C1AAA001-0029018) and (NRF-2014R1A2A1A11053567) for financial support of this work.

4. References

[1] S. Bai and X. Shen, *RSC Advances* 2012, **2**, 64-98.

[2] A.T. E. Vilian, S. Chen, L.Huang, M. Ajmal Ali, F. M.A. Al-Hemaid, *Electrochim. Acta* 2014, **125**, 503-509.

[3] M. Yola, T. Eren, N. Atar, *Electrochim. Acta* 2014, **125**, 38-47.

[4] A.T. E. Vilian, S. Chen, Y. Chen, M. Ajmal Ali, F. M.A. Al-Hemaid, *J. Colloid Interface Sci.* 2014, **423**, 33-40.

[5] Y. Zhu, S. Murali, W. Cai, X. Li, J. Suk, J. Potts and R. Ruoff, *Advanced Materials* 2010, **223**, 906-3924.

[6] Y. Shao, J. Wang, M. Engelhard , C. Wang and Y. Lin, *J. Mater. Chem.* 2010, **20**, 743-748.

[7] H. Guo, X. Wang, Q. Qian, F. Wang and X. Xia, *ACS Nano* 2009, **3**, 2653-2659.

[8] H. Filik, D. Aksu, R. Apak, İ. Şener, E. Kılıç, *Sens. Actuators B* 2009, **136**, 105-112.

[9] K. Venkatraman, The Chemistry of Synthetic Dyes, vol. I, Academic Press, New York, 1952, p. 184.

[10] H. Song, T.S. Chen, *J. Biochem. Mol. Toxicol.* 2001, **15**, 34-40.

[11] A. Yesilada, H. Erdogan, M. Ertan, *Anal. Lett.,* 1991, **24**, 129-138.

[12] T. Németh, P. Jankovics, J. Németh-Palotás, H. Ko˝ szegi-Szalai, *J. Pharm. Biomed. Anal.* 2008, **47**, 746-749.

[13] L. Monser, F. Darghouth, *J. Pharm. Biomed. Anal.* 2002, **27**, 851-860.

[14] F. Mohamed, M. AbdAllah, S. Shammat, *Talanta* 1997, **44** , 61-68.

[15] Q. Chu, L. Jiang, X. Tian, J. Ye, *Anal. Chim. Acta,* 2008, **606**, 246-251.

[16] H. Filik, D. Aksu, R. Apak, I. Şener, E. Kılıç, *Sens. Actuators B*, 2009, **136**, 105-112.

[17] A. Safavi, N. Maleki, O. Moradlou, *Electroanalysis* 2008, **20**, 2158-2162.

[18] H.Yin,Q. Ma, Y. Zhou, S. Ai, L. Zhu, *Electrochim. Acta* 2010, **55**, 7102- 7108.

[19] Y.Fan, J. Liu, C. Yang, M. Yu, P. Liu, *Sens. Actuators B* 2011, **157**, 669- 674.

[20] J. Neto, W. Santos, P. Lima, S. Tanaka, A. Tanaka, L. Kubota, *Sens. Actuators B* 2011, **152**, 220-225.

[21] L. Shiroma, M. Santhiago, A. Gobbi, L. Kubota, *Anal. Chim. Acta,* 2012, **725**, 44-50.

[22] C. De Bleye, E. Dumont, E. Rozet, P.Y. Sacré, P.F. Chavez, L. Netchacovitch, G. Piel, Ph. Hubert, E. Ziemons, *Talanta* 2013, **116**, 899-905.

[23] R. Wang, K. Yan, F. Wang, J. Zhang, *Electrochim. Acta* 2014, **121**, 102-108.

[24] A. T. E. Vilian and S. Chen, *RSC Adv*., 2014, **4**, 55867-55876.

[25] D. Marcano, D. Kosynkin, J. Berlin, A . Sinitskii, Z. Sun, A. Slesarev, L. Alemany, W .Lu, J. Tour, *Nano. Lett* 2010, **4**, 4806-4814.

[26] S. Pan and X. Liu, *New J. Chem*., 2012, **36**, 1781-1787.

[27] Y. Li, Q. Zhao, J. Ji , G. Zhang, F. Zhang and X. Fan, *RSC Adv*, 2013, **3**, 13655-13658.

[28] T-Y. Lin and D-H. Chen, *RSC Adv*., 2014, **4**, 29357-29364.

[29] S. Muralikrishna, K. Sureshkumar, T. S. Varley, D. H. Nagaraju and T. Ramakrishnappa, *Anal. Methods*, 2014, **6**, 8698-8705.

[30] S-j. Li, D-H Deng, H. Pang, L. Liu,Y. Xing, S. Liu,*J Solid State Electrochem* 2012, **16**, 2883-2889.

[31] D. Sun, X. Li, H. Zhang, X. Xie, *Int. J. Environ. Anal. Chem.* 2012, **92**, 324-333.

[32] M. Jamal, S.A. Sarac, E. Magner, *Sens. Actuators B* 2004, **97**, 59-66.

[33] Z. Wang, H. Zhu, H. Zhang, G. Gao, Z. Sun, H. Liu, X. Zhao, *Electrochim. Acta* 2009, **54**, 7531-7535.

[34] S. Mehretie, S. Admassie, T. Hunde, M. Tessema, T. Solomon, *Talanta* 2011, **85**, 1376-1382.

[35] W. Su, S. Wang, S. Cheng, *J. Electroanal. Chem.* 2011, **651**, 166-172.

[36] S. Duan, X. Zhang, S. Xu, C. Zhou, *Electrochim. Acta* 2013, **88**, 885-891.

[37] H. Filik, D. Aksua, R. Apaka, I. Sener, E. Kilic, *Sens. Actuators B* 2009, **136**, 105-112.

[38] H. Filik, M. Hayvalı, E. Kilic, R. Apaka, D. Aksua, Z. Yanaza, T. Cengel, *Talanta* 2008, **77**, 103-109.

[39]J. Neto, W. Santos, P. Lima, S. Tanaka, A. Tanaka, L. Kubota, *Sens. Actuators B* 2011, **152**, 220-225.

[40] R. Wang, K. Yan, F.Wang, J. Zhang, *Electrochim. Acta* 2014, **121**, 102-108.